Assessing the feasibility of mapping changes of ecosystem functional groups in South African estuaries using Landsat and Sentinel images of 1990, 2014, 2018 and 2020

Heidi van Deventer[1,2*](ORCID 0000-0002-7854-2155) · Philani Apleni [2] (ORCID 0000-0001-9280-7263) · Janine B Adams[3,4] (ORCID 0000-0001-7204-123X) · Taryn Riddin[3,4] (ORCID 0000-0002-5877-3431) · Emily Whitfield[3,4] (ORCID 0000-0002-6900-8823)· Anesu Machite[3,4] (ORCID 0000-0001-7489-6346) · Lara van Niekerk[1,3, 4] (ORCID 0000-0001-5761-1337) · Akhona Madasa[5]

1 Council for Scientific and Industrial Research (CSIR), PO Box 395, Pretoria 0001, Stellenbosch 7600. South Africa
2 Department of Geography, Geoinformatics & Meteorology, University of Pretoria, Private Bag X20, Hatfield, Pretoria 0028, South Africa
3 Department of Science & Innovation–National Research Foundation (DSI-NRF) Research Chair in Shallow Water Ecosystems, Department of Botany, Nelson Mandela University, South Africa
4 Institute for Coastal and Marine Research, Nelson Mandela University, South Africa
5 South African National Biodiversity Institute

* Correspondence: HvDeventer@csir.co.za; Tel.: (+27) 12 841 2507

Supplementary Information I

Table SI.I.1 Comparison of the extent of South African estuarine habitats and international estuarine ecosystem functional groups (EFGs) identified in the International Union for Conservation of Nature's (IUCN's) global ecosystem types (Keith et al. 2022). Estuarine blue carbon ecosystems are listed under two realms, including (a) M1 = marine shelves; and (b) MFT = Marine–freshwater–terrestrial. Within these two realms, three blue carbon ecosystem types are recognised, including MFT1.2 and 1.3 and M1.1)

Estuarine habitat (and comparable EFG name)	**Description of Ecosystem Functional Groups (Keith et al. 2022)**	**Global extent**	**Estuarine habitat (and comparable EFG name)**
Mangroves (MFT1.2 Inter-tidal forests and shrubland)	"Intertidal mangrove-dominated systems, producing high amounts of organic matter that is both buried in situ and exported; sediments dominated by detritivores and leaf shredders, with birds, mammals, reptiles and terrestrial invertebrates occupying the canopy". Distribution: "Tropical and warm temperate coastline with good	2 851 (South African extent, Bunting et al. [2022])	2 820 (Raw et al. 2023)

	sediment supply" (Keith et al. [2022]: Extended Table 4).		
Salt marshes (MFT1.3 Coastal saltmarshes and reedbeds)	"Variable salinity tidal system dominated by salt-tolerant plants, with invertebrates, small/juvenile fish and birds. Distribution: "Tropical and warm temperate coastline with good sediment supply" (Keith et al. [2022]: Extended Table 4).	8 973.8 (Worthington et al. 2023) 6 129.5 (McOwen et al., 2017) (no extent mapped in the Allen Coral Atlas [2020], only points)	14 713 (Raw et al. 2023)
Sand and mud banks (not listed as an IUCN EFG)	N.A. Mapped as part of South African estuaries habitat. Important habitat for benthic micro algae that is a key food source in estuaries.	N.A.	6 108 (sand & mudbanks, Adams et al. [2019])
Submerged macrophytes (M1.1 Seagrass meadows)	N.A. (Broad polygon mapped for offshore environment around Kosi Bay by Short et al. [2007], indicating a region of possible occurrence, rather than true extent).	41 000 as Seagrasses (Short et al. [2007])	1 755 as Seagrasses & sub-merged macrophytes (Raw et al. [2023])

Supplementary Information II

South Africa's 332 estuarine systems occur across four original bioregions of the estuaries, ranging from the western coastline eastwards as cool temperate, warm temperate, subtropical and tropical (Van Niekerk et al. 2019). These bioregions were further subdivided for the purpose of reporting to which degree estuarine habitats were mapped for different parts of the coast. The cool temperate bioregions were divided into a cool temperate arid (northern) and Mediterranean (southern) coastal regions; the warm temperate bioregion was divided between those areas with and without mangroves, whereas the subtropical and tropical estuaries were reported together in the subtropical coastal regions. This resulted in five coastal regions of reporting used in Fig. 1 of the main text. The results showed that most estuarine habitats were manually mapped after the year 2004, with Swartvlei and the Touw/Wilderness estuaries being the only two mapped in 1998 (Table SI.II.1). Initially, during the first ten years (1998 and 2009), many studies focused on the Warm temperate coastal region where mangroves do not naturally occur, while an increase in representation across all five coastal regions took place after 2013. A marked increase in the number of estuarine systems with estuarine habitat maps are noted for 2019, and 2020, with >10 estuaries with habitat maps now represented. This progress has enabled between 68-100% of the number of estuaries being mapped for the cool temperate arid, cool temperate Mediterranean and warm temperate coastal regions. The two coastal regions with mangroves, however, show a need for improved representation of the number of estuaries mapped, including the warm temperate with mangroves coastal region (only 34% of the number of estuarine systems have habitat maps) and the subtropical coastal region (only 23%) (Table SI.I.1).

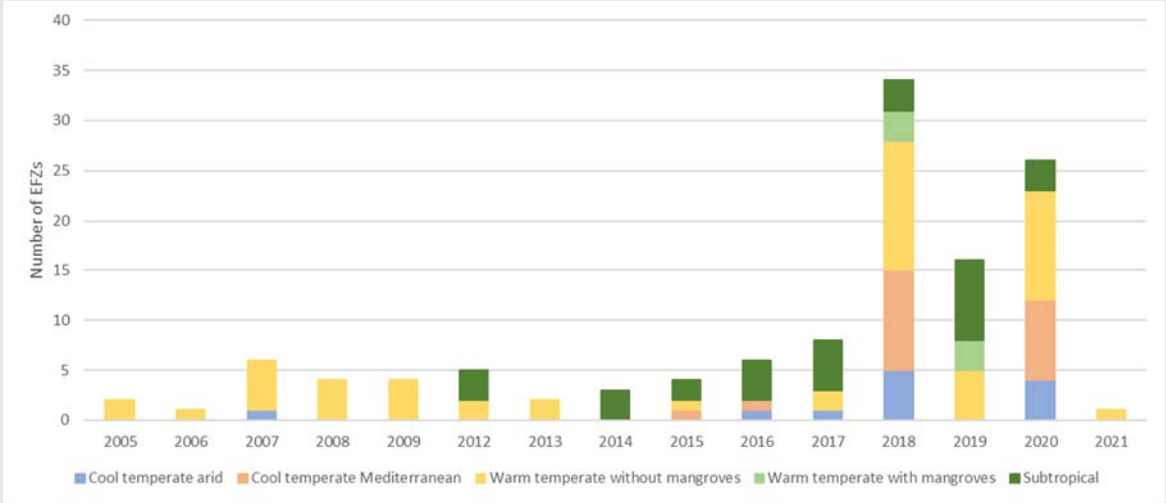

Fig. SI.II.1. Number of South Africa's estuaries for which estuarine habitats were mapped across five coastal regions and years.

Table SI.II.1. Number and percentage of estuaries (*n*=290) mapped across years and the five coastal regions. Micro-estuaries have not yet been mapped to date

Year	Cool temperate arid	Cool temperate Mediterranean	Warm temperate without mangroves	Warm temperate with mangroves	Sub-tropical	Total number
Total number of estuaries per Earth Observation subregion	10	22	81	44	133	290
1998			2			2
2004			1			1
2005	1		5			6
2006			4			4
2007			4			4
2008			2		3	5
2009			2			2
2012					3	3
2013		1	1		2	4
2014	1	1			4	6
2015	1		2		5	8
2016	5	10	13	3	3	34
2017			5	3	8	16
2018	4	8	11		3	26
2019			1			1
2020	1	2	2	2	1	8
2021	3	2	24	11	16	56
Total number of estuaries mapped (percentage of total)	10 (100%)	16 (73%)	55 (68%)	15 (34%)	30 (23 %)	126 (43 %)

Supplementary Information III:

Extended description of the steps taken to generating Regions of Interest (ROIs) for remote sensing classification of estuarine ecosystem functional groups. This phase consisted of four subphases as per Fig. 2, with a description of the relevant steps undertaken under each phase as follows:

(a1) Automated extraction of points from the Nelson Mandela University (NMU) habitat types

Initially a set of sample points was generated from the existing NMU National Botanical database polygon layer (Adams et al. 2016, 2019) for use in the remote sensing classification. The coastal regions were divided among the team members to facilitate the validation in Google Earth Pro images (GEP 1985-2022) across multiple years. The steps taken included:

- The estuarine polygons were extracted from the National Wetland Map Version 5 (NWM5; Van Deventer et al. 2020), the inland section of the estuarine system was kept while the shore regions (Harris et al. 2019) were removed, and the inland section buffered with 50 m;
- The polygons were unioned with the habitat types of 2021/11/25 from NMU in ArcGIS 10.7 (ESRI 1999–2018);
- The extent of each estuarine system was divided by 20x20 m (400 m²) and representative sample points generated for areas where the Macrophyte class of NMU dataset covers such extents, and the EFG type could be extracted and used in remote sensing classification;
- Sample points were generated based on the extent "Hab_ext_m2" field and a minimum distance of 100 m between points, resulting in the field "Nr_samples", that shows the maximum number of sample points possible for that polygon;
- The estuarine boundaries and habitats were converted to lines and all sample points generated that were located within 20 m of these lines, were removed to avoid inclusion of spectra on transitional edges of classes;
- The habitat classes were then extracted for the remaining points, translated to the EFG classes, converted to kml format, for validation and added to in Google Earth Pro; and
- An Excel spreadsheet with the unique numbers of the sample points was shared between the team for defining the EFGs per year, and a note field to indicate confidence and other issues.

(a2) Validation of sample points using Google Earth Pro images

During the validation process, the following criteria was taken into consideration:

(i) A pixel that was selected for an ROI should be homogenous for the full pixel size, and ideally also all adjacent pixels around this selected one. Therefore, if using Sentinel–2 at a 10 m spatial resolution, a centre pixel could be identified as an ROI, if it is at the centre of an area of at least 30 x 30 m of homogenous cover.

(ii) Where a single pixel was selected as an ROI, at least >80% of the extent of the pixel should have been related to a single class.

(iii) ROIs selected for vegetation classes, should not have had background influence from water, sand, mud or other backgrounds, otherwise this would have resulted in high spectral confusion between different classes, and low overall and user accuracy values (used to evaluate and approve results).

(iv) Mixed vegetation classes, such as "Mixed reeds, sedges and mangroves", were avoided, and ideally split into either "Mangroves" and "Reeds and Sedges". The latter two were envisaged as classes with clear dominance of these canopies for >80% of the extent of a 10x10 m pixel.

(v) ROIs should not be near ecotonal changes or other classes. Such ROIs should have been moved >20 m away from ecotonal changes from one class to another, and rather select or position it where there was a high confidence in a class.

(a3) Capturing of additional samples points in Google Earth Pro for selected classes

A number of classes were identified as estuarine EFG subtypes where subdivision of the main EFGs and additional ROIs were added to the extracted points. These included:

- Intertidal salt marsh (*Spartina maritima*)
- Intertidal salt marsh (Succulent)
- Submerged macrophytes (intertidal *Zostera*)
- Submerged macrophytes (subtidal *Zostera*)
- Supratidal salt marsh (*Juncus kraussii*)
- Supratidal salt marsh (Other)
- Supratidal salt marsh (Saline grasses)

These classes are generally narrow in extent and in some instances also ephemeral, especially *Zostera capensis*, where changes in estuarine hydrological dynamics may result in changes in the extent and location of these systems. These submerged macrophytes also may be very dynamic over hydrological and tidal regimes, sensitive to changes in mouth state and

may vary geographically as a result of natural and other pressures. Some of these classes also consist of a mosaic of mixed vegetation and do not have homogenous, dense canopies.

(a4) Spatial integration and translation of sample point classes from all datasets to a single file per year with consistent class names

Based on the initial outputs, a review was done of the existing points and further sample points were captured for the estuarine system.

Supplementary Information IV:

SI.IV.1. Selection and pre-processing of satellite images

Google Earth Engine (GEE; Gorelick et al. 2017) was chosen as the platform to process the outputs, considering the capabilities of this cloud-computing platform in managing extensive areas and number of images, compared to individual desktop machines. The pre-processing of the Landsat series of images, and the Sentinel–1 and –2 datasets, were done as follows:

(i) Pre-processing of Landsat optical images in GEE

GEE has a Landsat Surface Reflectance collection that has undergone the required pre-processing of the optical images for classification. This includes atmospheric correction, georeferencing, orthorectification and resampling to the 30-m spatial resolution of the visible bands. Bands included in the remote sensing classification were the optical (2, 3, 4), the near-infrared (NIR; 5), the two Shortwave Infrared (SWIR; 6 & 7) and Thermal Infrared (TIR) bands;

(ii) Pre-processing of Sentinel-1 radar images in GEE

Images from the twin-sensors Sentinel-1A and Sentinel-1B in interferometric wide-swath mode (IW) were considered for the remote sensing classification. The GEE collection includes both the Vertical-Vertical (VV) and Vertical Horizontal (VH) Ground Range Detected (GRD) images (Gorelick et al. 2017). Pre-processing was done according to the recommended steps of Mullissa et al. (2021), including border noise correction, speckle filtering and radiometric terrain normalisation (Apleni in prep); and

(iii) Pre-processing of Sentinel-2 optical images in GEE

This sensor also has a twin constellation, Sentinel-2A and -2B, providing four 10-m spatial resolution spectral bands in the visible region, six 20-m spatial resolution bands in the red-edge, NIR and SWIR regions, and three 60-m spatial resolution bands that is used for atmospheric correction. The image collection in GEE for Sentinel-2 includes atmospheric correction, georeferencing, orthorectification and resampling to a 10-m spatial resolution. In addition, clouds and cloud shadows were masked with the use of the Quality Assurance band 60 (QA60 band).

GEE was used to generate composites of images for the main EO regions (those with mangroves or without), to enable the compilation of composite subsets for each of these tiles, and then generate a single composite of all the images for each EO

region. The tiled composites of the S1+S2 images were used for the classification of the years 2018 and 2020 and reported here.

SI.IV.2 Inclusion of indices and topographic data to optimise the classification accuracies

To optimise the classification accuracies of the EFGs, additional spectral indices and ratios and topographic data, together with ancillary data were combined with the image composites for the classification. These have been previously proven through several studies globally to enhance classification accuracies of wetland vegetation (e.g., Van Deventer et al. 2022). Eleven spectral indices were derived from the Landsat and Sentinel optical sensors, whereas the Sentinel-1 ratio was derived from the VV and VH backscatter information of this radar satellite (Table SI.IV.1). Elevation of the estuaries was included in the classification using the 30 m spatial resolution National Aeronautics and Space Administration (NASA) Digital Elevation Model (DEM) data (Buckley et al. 2020). The NASA DEM combines data from the Shuttle Radar Topography Mission (SRTM), the Advanced Spaceborne Thermal Emission and Reflection Radiometer (ASTER), Global Digital Elevation Model (GDEM), Ice, Cloud, and Land Elevation Satellite (ICESat), Geoscience Laser Altimeter System (GLAS), and Panchromatic Remote Sensing Instrument for Stereo Mapping (PRISM) to ensure no gaps and improve the spatial accuracy (Farr et al. 2007; Buckley et al. 2020). In addition, topographic data were derived from the NASADEM, including degrees of slope and aspect, which were also included in the stacked, with the indices and band composites for the classification.

Table SI.IV.1. Vegetation and water indices included in the classification of the estuarine Ecosystem Functional Groups (EFGs) to enhance the separability of the remote sensing classes. NIR = near infrared; SWIR = Shortwave infrared

Spectral index	Equation	Wetland property enhanced
Difference Vegetation Index (DVI) (Tucker 1979)	$DVI = \mathrm{NIR} - \mathrm{Red}$	Soil Moisture
Enhanced Vegetation Index (EVI) (Huete et al. 2002)	$EVI = 2.5 \times \frac{(\mathrm{NIR} - \mathrm{Red})}{(\mathrm{NIR} + (6 \times \mathrm{Red} - 7.5 \times \mathrm{Blue}) + 1}$	Chlorophyll
Green Difference Vegetation Index (GDVI) (Tucker 1979)	$GDVI = \mathrm{NIR} - \mathrm{Green}$	Chlorophyll and nitrogen
Green Normalized Difference Vegetation Index (gNDVI) (Gitelson et al. 1996)	$gNDVI = \frac{(\mathrm{NIR} - \mathrm{Green})}{(\mathrm{NIR} + \mathrm{Green})}$	Chlorophyll
Green Soil Adjusted Vegetation Index (GSAVI) (Mahdianpari et al. 2020; Sripada 2005)	$gSAVI = \frac{(\mathrm{NIR} - \mathrm{Green})}{(\mathrm{NIR} + \mathrm{Green}) + 0.5} \times 1.5$	Chlorophyll
Modified Normalized Difference Water Index (MNDWI) (Xu 2006)	$MNDWI = \frac{(Green - \mathrm{SWIR})}{(Green + \mathrm{SWIR})}$	Leaf water content
Modified Soil Adjusted Vegetation Index (MSAVI) (Qi et al. 1994)	$MSAVI = \frac{2\mathrm{NIR} + 1 - \sqrt{(2\mathrm{NIR} + 1)^2} - 8(NIR - Red)}{2}$	Chlorophyll
Normalized Difference Vegetation Index (NDVI) (Rouse et al. 1973; Tucker 1979)	$NDVI = \frac{(\mathrm{NIR} - \mathrm{Red})}{(\mathrm{NIR} + \mathrm{Red})}$	Chlorophyll
Normalized Difference Water Index (NDWI) (Gao 1996)	$NDWI = \frac{(R\mathrm{NIR} - R\mathrm{SWIR})}{(R\mathrm{NIR} + R\mathrm{SWIR})}$	Leaf & water content
Optimized Soil Adjusted Vegetation Index (OSAVI) (Rondeaux et al. 1996)	$OSAVI = \frac{(\mathrm{NIR} - \mathrm{Green})}{(\mathrm{NIR} + \mathrm{Red}) + 0.16}$	Chlorophyll and leaf area Index

Red Edge Normalized Difference Vegetation Index (NDVIre); (Gitelson and Merzlyak 1994)	$NDVIre = \frac{(\text{NIR} - \text{Red Edge})}{(\text{NIR} + \text{Red Edge})}$	Chlorophyll, leaf area/ biomass and nitrogen
Sentinel-1 ratio (Greifeneder et al. 2018)	$Sratio = \frac{\text{VV}}{\text{VH}}$	Vegetation structure

References

Buckley SM, Agram, PS, Belz JE, Crippen RE, Gurrola EM, Hensley S, Kobrick M, Lavelle M, Martin JM, Neumann M, Nguyen QD, Rosen PA, Shimada JH, Simard M, Tung WW (2020) NASADEM. National Aeronautics and Space Administration Jet Propulsion Laboratory, California Institute of Technology, Pasadena, California, United States of America. https://portal.opentopography.org/datasetMetadata?otCollectionID=OT.032021.4326.2.

Environmental Systems Research Institute (ESRI) (1999–2018). ArcGIS desktop 10.7, Redlands, CA, ESRI, United States of America. https://www.esri.com/en-us/home.

Farr TG, Rosen PA, Caro E, Crippen R, Duren R, Hensley S, Kobrick M, Paller M, Rodriguez E, Roth L, Seal D, Shaffer S, Shimada J, Umland J, Werner M, Oskin M, Burbank D, Alsdorf D (2007) The Shuttle Radar Topography Mission. Rev Geophys 45(2), 1–33. https://agupubs.onlinelibrary.wiley.com/doi/10.1029/2005RG000183; Data DOI: https://doi.org/10.1029/2005RG000183.

Gao B-C (1996) NDWI – A normalized difference water index for remote sensing of vegetation liquid water from space. Remote Sens Environ 58, 257–266. https://www.sciencedirect.com/science/article/pii/S0034425796000673; Data DOI: https://doi.org/10.1016/S0034-4257(96)00067-3.

Google Earth Pro (GEP) Version 7.3.3.7786 (1985–2022). Various images composites available in GEP for the Estuarine Functional Zones of South Africa. Available from the server kh.google.com and http://www.earth.google.com.

Gitelson A, Merzlyak MN (1994) Spectral reflectance changes associated with autumn senescence of *Aesculus hippocastanum* L. and *Acer platanoides* L. leaves. Spectral features and relation to chlorophyll estimation. J Plant Physiol 143(3), 286–292.

Gitelson AA, Kaufman YJ, Merzlyak MN (1996) Use of a green channel in remote sensing of global vegetation from EOS-MODIS. Remote Sens Environ 58(3), 289–298. https://www.sciencedirect.com/science/article/pii/S0034425796000727; Data DOI: https://doi.org/10.1016/S0034-4257(96)00072-7.

Greifeneder F, Notarnicola C, Hahn S, Vreugdenhil M, Reimer C, Santi E, Paloscia S, Wagner W (2018) The Added Value of the VH/VV Polarization-Ratio for Global Soil Moisture Estimations from Scatterometer Data. IEEE J Sel Top Appl Earth Obs 1–12. https://doi.org/10.1109/jstars.2018.2865185.

Harris LR, Bessinger M, Dayaram A, Holness S, Kirkman S, Livingstone T-C, Lombard AT, Lück-Vogel M, Pfaff M, Sink KJ, Skowno AL, Van Niekerk L (2019) Advancing land-sea integration for ecologically meaningful coastal conservation and management. Biol Conserv 237, 81–89. https://www.sciencedirect.com/science/article/pii/S0006320719302939; Data DOI: https://doi.org/10.1016/j.biocon.2019.06.020.

Huete A, Didan K, Miura T, Rodriguez EP, Gao X, Ferreira LG (2002) Overview of the radiometric and biophysical performance of the MODIS vegetation indices. Remote Sens Environ 83(1–2), 195–213. Available via DIALOG: https://www.sciencedirect.com/science/article/pii/S0034425702000962; Data DOI: https://doi.org/10.1016/S0034-4257(02)00096-2.

Jarvis A, Reuter HI, Nelson A, Guevara E (2008) Hole-filled SRTM for the globe Version 4, available from the CGIAR-CSI SRTM 90m Database. https://srtm.csi.cgiar.org.

Mullissa A, Vollrath A, Odongo-Braun C, Slagter B, Balling J, Gou Y, Gorelick N, Reiche J (2021) Sentinel-1 SAR backscatter analysis ready data preparation in google earth engine. Remote Sens 13(10), 1954. https://www.mdpi.com/2072-4292/13/10/1954; Data DOI: https://doi.org/10.3390/rs13101954.

Qi J, Chehbouni A, Huete AR, Kerr YH, Sorooshian S (1994) A modified soil adjusted vegetation index. Remote Sens Environ 48(2), 119–126. https://www.sciencedirect.com/science/article/abs/pii/0034425794901341; Data DOI: https://doi.org/10.1016/0034-4257(94)90134-1.

Rondeaux G, Steven M, Baret F (1996) Optimization of soil-adjusted vegetation indices. Remote Sens Environ 55(2), 95–107. https://www.sciencedirect.com/science/article/pii/0034425795001867; Data DOI: https://doi.org/10.1016/0034-4257(95)00186-7.

Rouse J, Hass R, Schell J, Deering D (1973) Monitoring vegetation systems in the Great Plains with ERTS. Third ERTS Symposium, NASA, SP–351 I, 309–317. https://ntrs.nasa.gov/archive/nasa/casi.ntrs.nasa.gov/19740022614.pdf.

Sripada R (2005) Determining In-Season Nitrogen Requirements for Corn Using Aerial Color-Infrared Photography. Ph.D. dissertation, North Carolina State University. https://repository.lib.ncsu.edu/handle/1840.16/4200.

Tucker CJ (1979) Red and Photographic Infrared Linear Combinations for Monitoring Vegetation. Remote Sens Environ 8(2), 127–150. https://www.sciencedirect.com/science/article/abs/pii/0034425779900130; Data DOI: https://doi.org/10.1016/0034-4257(79)90013-0.

Xu H (2006) Modification of normalised difference water index (NDWI) to enhance open water features in remotely sensed imagery. Int J Remote Sens 27(14), 3025–3033. https://www.tandfonline.com/doi/full/10.1080/01431160600589179; Data DOI: https://doi.org/10.1080/01431160600589179.